

Article

Investigating the Role of Cs Species in the Toluene–Methanol Side Chain Alkylation Catalyzed by CsX Catalysts

Zhihui Zhang ^{1,*} , Qingwei Wang ¹, Wenxiu Gao ¹, Chunxiang Ma ² and Miaomiao Yang ¹

¹ College of Chemical and Pharmaceutical Engineering, Jilin Institute of Chemical Technology, Jilin 132022, China; wqw15643590515@163.com (Q.W.); gaowenxiu-0922@jlicet.edu.cn (W.G.); ymm19990557619@163.com (M.Y.)

² Research Institute of PetroChina Jilin Petrochemical Company, Jilin 132022, China; jh_macx@petrochina.com.cn

* Correspondence: zhangzh@jlicet.edu.cn; Tel.: +86-432-15004326878

Abstract: The side chain alkylation of toluene with methanol was studied on a series of CsX catalysts prepared by varying the Cs species and ion exchange conditions. The effects of various parameters, such as the exchanging temperatures and times on the adsorption/activation properties of different CsX catalysts, were investigated by combining a variety of characterization means for understanding the role of Cs species in the side chain alkylation reaction. On the basis of the various characterization results and their related literature results, it can be proposed that the Cs ions located on the ion-exchanged sites of X zeolites could effectively adsorb and activate toluene molecularly through modifying the basicity of framework oxygen, whereas the cluster of cesium oxide (Cs₂O) could ensure the effective conversion of methanol into formaldehyde. Additionally, Cs ions can promote the production of monodentate formate, which enhances the selectivity of styrene. However, too much Cs₂O will lead to the excessive decomposition of methanol into CO₂, CO, and H₂, thus inhibiting the production of styrene. In summary, the presence of suitable amounts of Cs ions and Cs₂O clusters plays a significant role in the formation of the side chain products of styrene and ethylbenzene.

Keywords: toluene; methanol; side chain alkylation; cesium (Cs); CsX zeolite



Citation: Zhang, Z.; Wang, Q.; Gao, W.; Ma, C.; Yang, M. Investigating the Role of Cs Species in the Toluene–Methanol Side Chain Alkylation Catalyzed by CsX Catalysts. *Catalysts* **2024**, *14*, 256. <https://doi.org/10.3390/catal14040256>

Academic Editor: Giuseppe Bonura

Received: 18 February 2024

Revised: 30 March 2024

Accepted: 8 April 2024

Published: 12 April 2024



Copyright: © 2024 by the authors. Licensee MDPI, Basel, Switzerland. This article is an open access article distributed under the terms and conditions of the Creative Commons Attribution (CC BY) license (<https://creativecommons.org/licenses/by/4.0/>).

1. Introduction

Ethylbenzene and styrene are essential raw materials in the production of various important chemical products [1–4]. In industrial environments, styrene is primarily manufactured through the alkylation of benzene and ethylene to produce ethylbenzene, followed by the dehydrogenation of ethylbenzene. However, this method presents several challenges, including its high energy consumption, complex process flow, and high production costs. Research has shown that toluene and methanol can undergo a side chain alkylation reaction with the aid of catalysts such as alkaline zeolites, resulting in the direct synthesis of styrene. Especially for cesium-modified zeolite X or Y, it has been studied extensively and deeply. Two common techniques for incorporating cesium into zeolites are ion exchange and impregnation. Due to the dissimilarities between these methods, cesium typically exists in diverse forms.

Borgna et al. [5] found that a Cs ion-exchanged NaX catalyst started to generate side chain alkylation products when the Cs content exceeded 18%. Moreover, when the Cs content was higher than 31%, the Cs ion-exchanged NaY zeolite catalyst predominantly underwent side chain alkylation. Similar studies were conducted by using K ion-exchanged NaX zeolites [6]. Using the cesium ion exchange technique, it is possible to substitute sodium ions in zeolite X or Y with cesium ions to a certain extent or even entirely. There are diverging views among researchers regarding the existence of Cs. Some argue that Cs exists in the form of Cs⁺ [7], while others propose that it exists in the form of oxide clusters [8,9]. According to a study by Palomares [10], the presence of cesium ions within the framework

not only enhances the strength of the catalyst's base but also stabilizes the adsorption of toluene. Modifications of Cs and other alkali metals can significantly improve the alkalinity of the zeolite. However, an excessively basic catalyst can lead to excessive decomposition of methanol, which hinders the progress of side chain alkylation [11–13]. A catalytic system with exceptional performance for side chain alkylation reactions should exhibit a synergistic effect at the acid–base center, which contributes to the controlled reaction rate [14,15]. Based on the findings of Unland, Baker, Lin, and Sphon [16], the creation of styrene may be facilitated through the utilization of modified zeolite X or Y, specifically by incorporating boron or phosphorus ions through ion exchange. Hong et al. [17,18] incorporated the ammonia pool effect in Cs-modified X zeolites and Cs-modified X zeolites with the assistance of basic picoline as a co-catalyst, effectively neutralizing the excessively strong basic center and enhancing the yield of styrene. Our early research has yielded comparable outcomes [19,20].

In addition, some researchers have employed impregnation to modify X zeolites. According to common belief, impregnation can produce a zeolite catalyst with higher basicity, where the Cs species is present as Cs_2O . This leads to a significant enhancement in the conversion of side chain alkylation, but it also results in poor selectivity for styrene [8,13,21].

Despite the work mentioned above, there is still a need for a more comprehensive investigation into the specific impact of cesium content, forms of cesium species, and cesium species on the catalyst. Specifically, further research is required to understand the promotion effects of the reaction mechanism involved in the side chain alkylation of toluene using CsX.

To systematically investigate the influence of the preparation parameters on the Cs content and distribution state in the catalyst and the properties of the acid–base center, several experiments were conducted in this study. Different catalysts were prepared by varying the ion exchange conditions, and the effects of several parameters, such as the exchange temperature and time on the Cs content and distribution and the acid–base properties of the catalyst, were investigated. When the degree of Cs ion exchange is low, Cs species primarily exist in the form of Cs_2O on the outer surface of the molecular sieve. This promotes the formation of the active intermediate monodentate formate. However, an excessive amount of Cs_2O leads to the excessive decomposition of methanol into CO_2 and CO. As the degree of ion exchange increases, Cs enters the zeolite cage as Cs ions and acts as a Lewis acid center for stable adsorption of activated toluene and the alkylating reagent, i.e., monodentate formate. In addition, in situ infrared spectroscopy of methanol adsorption and TPD-mass spectrometry (MS) were employed to study the adsorption and activation of methanol on different types of CsX zeolite catalysts. A higher Cs^+ content promotes the generation of the active intermediate monodentate formate. Additionally, Cs^+ ions can effectively adsorb monodentate formate, thereby enhancing the methanol utilization rate and facilitating the production of styrene.

2. Results

2.1. Characterization of the Structure and Acid–Base Properties of CsX

2.1.1. X-ray Diffraction (XRD) Characterization

The XRD patterns of recently synthesized zeolites such as NaX and CsX are shown in Figure 1. Compared with that of NaX, the XRD peak intensity of CsX is noticeably decreased. This reduction in intensity can be attributed to the damage caused to the skeletal structure of the zeolite during the Cs ion exchange process, which leads to a decrease in the crystallinity of the zeolite. A comparison between the XRD spectra of the different CsX zeolites reveals significant differences in the intensities of the diffraction peaks. Notably, the diffraction peak intensities of the CsX_18 and CsX_37 zeolites are weaker than those of the other CsX zeolites. This phenomenon may be attributed to the higher ion exchange temperature (90 °C), which results in a more significant degradation of the skeletal structure of the zeolite. Additionally, the CsX zeolite exhibits distinct peaks at approximately 12.3° and 25.6°; the peak at 12.3° is attributed to cesium silicate-like species, and the peak at 25.6°

is attributed to Cs_2O . The XRD results in this study show that the CsX catalyst is prepared using the ion exchange method, with CsNO_3 serving as the source of cesium. The CsX catalyst contains cesium in three different forms: (1) Cs ions within the zeolite cage; (2) Cs^+ ions interacting with defective sites in the zeolite framework, leading to the formation of cesium silicate-like species or causing slight changes in the zeolite's structure (12.3°) [22]; and (3) highly dispersed Cs_2O (PDF no. 09-0104) on the surface of the zeolite, forming Cs_2O (25.6°) [7]. Note that Cs_2O is highly reactive and reacts with CO_2 and H_2O in the air when exposed to them for a prolonged period of time.

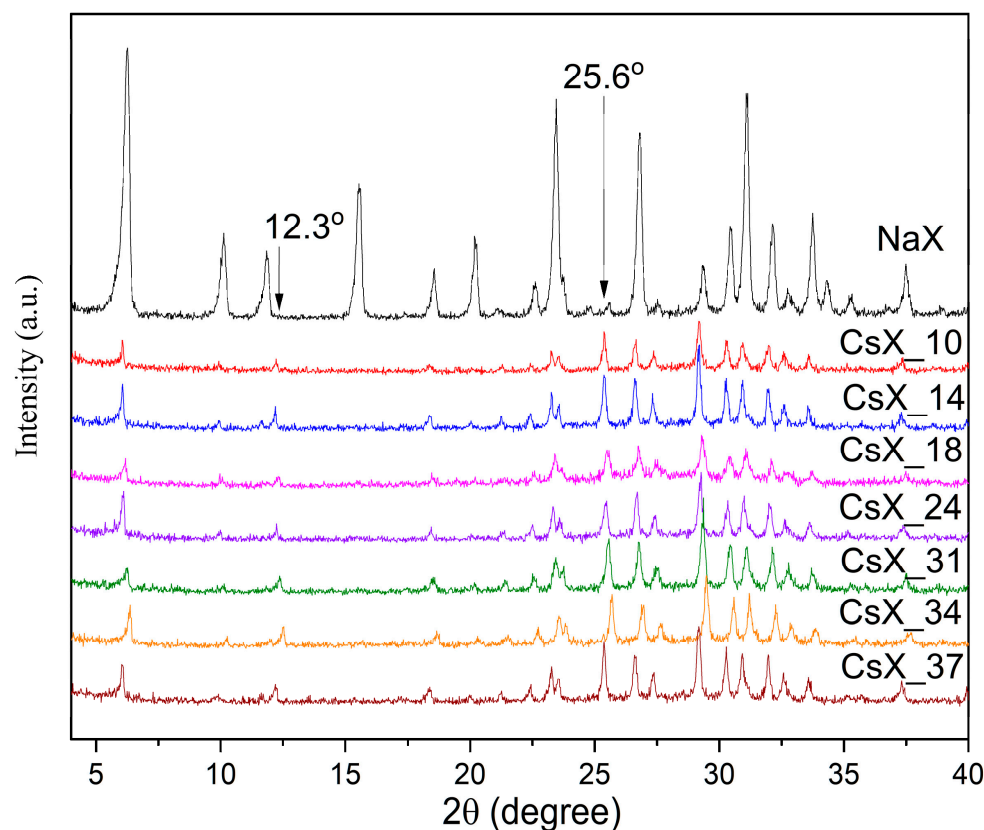


Figure 1. XRD patterns of the catalysts.

2.1.2. Analysis of Cs Content and Specific Surface Areas in CsX

The Cs content of the CsX zeolite was measured using ICP. Table 1 presents the mass percentage content and specific surface area of Cs in the different CsX zeolites. As the ion exchange temperature increases, the Cs content in CsX gradually rises. Additionally, CsX, which undergoes ion exchange twice, exhibits a higher Cs content. Following the introduction of Cs^+ ions, the specific surface area of the molecular sieves is notably decreased compared to that of NaX. However, the specific surface areas of CsX molecular sieves with varying Cs contents show minimal differences. This phenomenon could be attributed to the larger ionic radius of Cs^+ ions, which obstructs some of the pore channels in the molecular sieve, leading to the predominant distribution of Cs species on the outer surface of the molecular sieve.

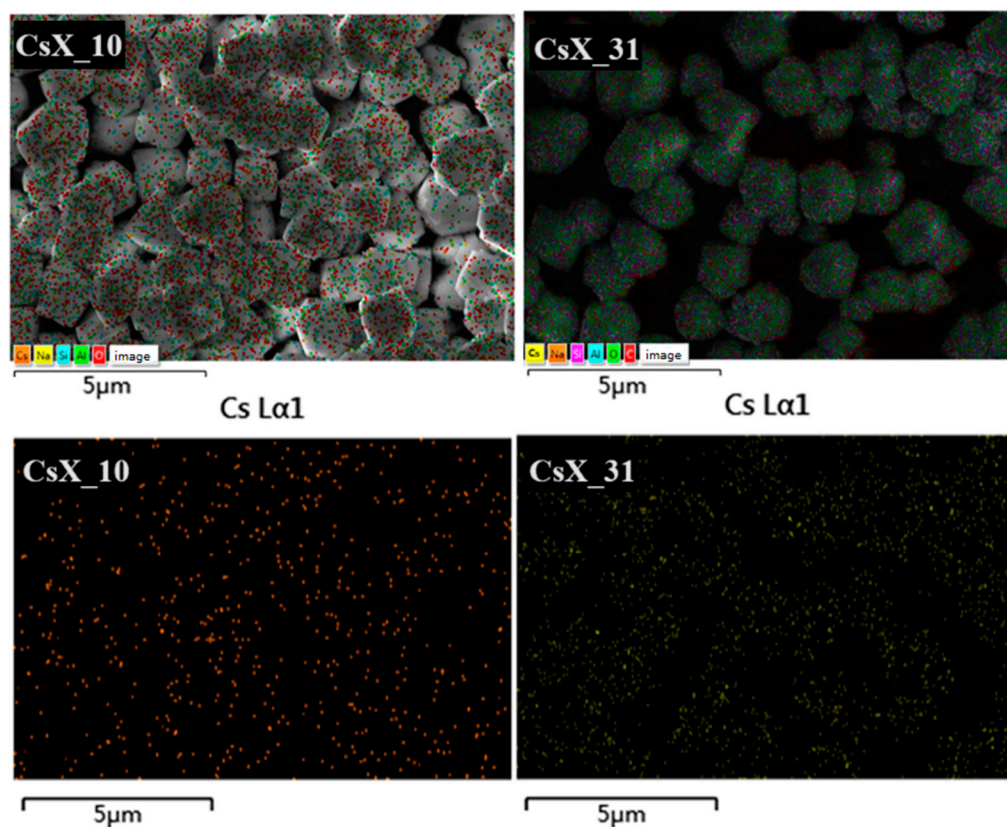
Table 1. Physicochemical characteristics of CsX zeolites.

Zeolite	Alkali Metal Content (wt%)		Exchange Degree ^b (%)	BET Surface Area (m ² ·g ⁻¹)	D _{Cs₂O} ^c
	Na ^a	Cs ^a			
NaX	14.09	--	--	677	--
CsX_10	11.02	10.12	13.7	351	51
CsX_14	9.96	14.23	19.8	351	52
CsX_18	8.90	18.19	26.1	352	55
CsX_24	7.65	24.04	35.2	328	60
CsX_31	5.63	31.78	49.4	341	65
CsX_34	4.65	34.21	56.0	349	69
CsX_37	3.91	37.83	62.6	386	76

^a Obtained from ICP results. ^b Calculated according to the following formula: Exchange degree = $\frac{\text{Cs content in one unit cell}}{\text{Cs content in one unit cell} + \text{Na content in one unit cell}}$. ^c The size of Cs₂O (D_{Cs₂O}) was determined from the Scherrer equation.

2.1.3. Scanning Electron Microscopy (SEM) Characterization

Figure 2 illustrates the distribution of Cs elements on the surfaces of the CsX_10 and CsX_31 zeolites; a uniform dispersion without noticeable agglomeration is observed. Figure 3 displays the SEM images of both the NaX and CsX zeolites, showing their regular crystal morphology. Table 2 showcases the findings of the SEM energy spectroscopy analysis, demonstrating the elemental composition of the NaX and CsX zeolites. With the rise in ion exchange temperature and the number of exchanges, there is a gradual increase in Cs content. The relatively consistent textural parameters of these catalysts provide further evidence that the crystal structure of X zeolites is maintained after introducing a certain amount of Cs species. The level of crystallinity is high, and the crystal particle size mainly falls within the range of 2–3 μm.

**Figure 2.** Distribution of Cs elements on CsX_10 and CsX_31.

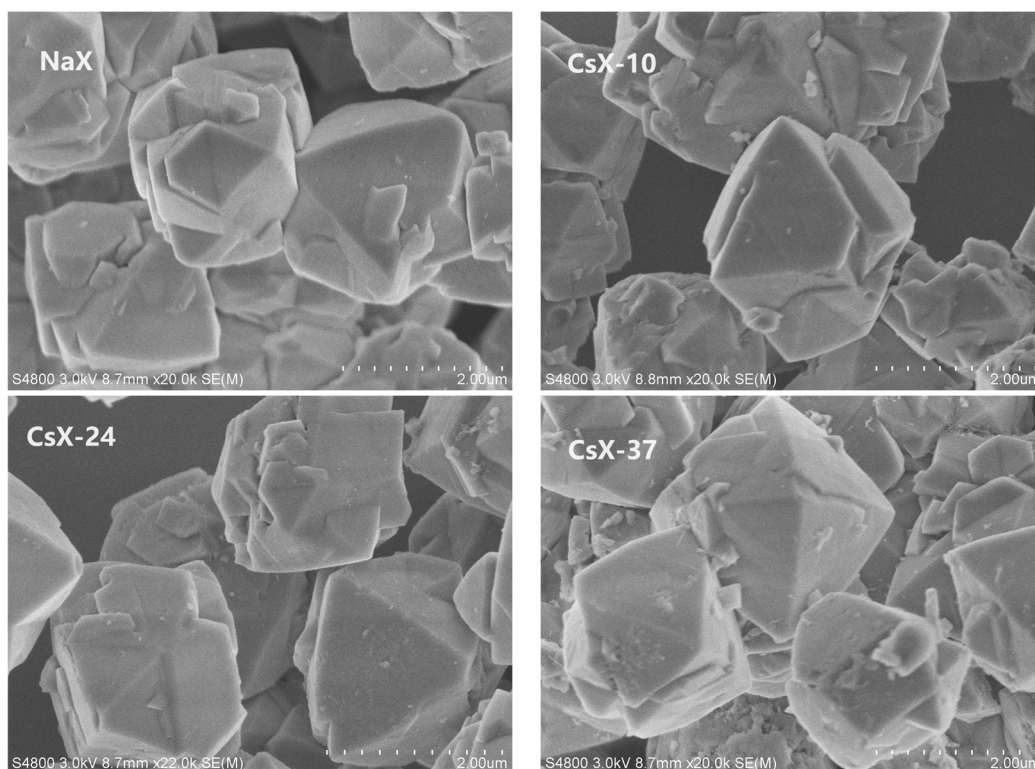


Figure 3. SEM images of NaX and CsX zeolites.

Table 2. SEM energy-dispersive spectrometry of NaX and CsX.

Zeolite	Chemical Composition (wt%) ^a				
	Cs	Si	Na	Al	O
NaX	--	23.5	10.6	18.8	47.1
CsX_10	13.3	12.5	10.1	24.1	40.0
CsX_14	14.5	12.5	9.2	24.1	39.7
CsX_18	17.6	12.1	8.6	23.2	38.5
CsX_24	23.3	11.3	7.5	21.7	36.2
CsX_31	31.9	10.2	5.3	19.7	32.9
CsX_34	35.3	9.9	4.2	19.0	31.7
CsX_37	35.2	10.0	3.7	19.2	31.9

^a Cs and Fe element distributions on zeolites derived from the EDS mapping.

The SEM images of CsX_24 and CsX_37 reveal that a small amount of fine particles (smaller than 0.5 μm) are attached to the surface of larger zeolite grains. These small particles may contain debris from the X zeolite crystallites and CsO species. Furthermore, the regularity of the CsX_37 crystal morphology is poor, suggesting that higher ion exchange temperatures can affect the morphology and particle size of zeolite crystals. These results demonstrate that when CsX is prepared via Cs^+ ion exchange, the Cs species are uniformly distributed across the surface and pores of the X zeolite. Although there are slight changes in the crystal morphology and structure of the zeolite, its main structure remains essentially unchanged.

2.1.4. Characterization of Acid–Base Center Properties

Figure 4 presents the NH_3 -TPD spectra of CsX; the main NH_3 desorption peak appears at approximately 206 $^\circ\text{C}$. This peak suggests the presence of medium-strength acidic centers on the surface of the zeolites. As the Cs content increases, the intensity of the acidic centers remains relatively stable, while the number of acidic centers gradually decreases. The

presence of cesium oxide, tentatively formed in the zeolite, affected the acidity of the original material. When modifying molecular sieves with CsNO_3 , the reduction in acid sites can be attributed to the basic nature of the CsNO_3 aqueous solution, which neutralizes the acid sites.

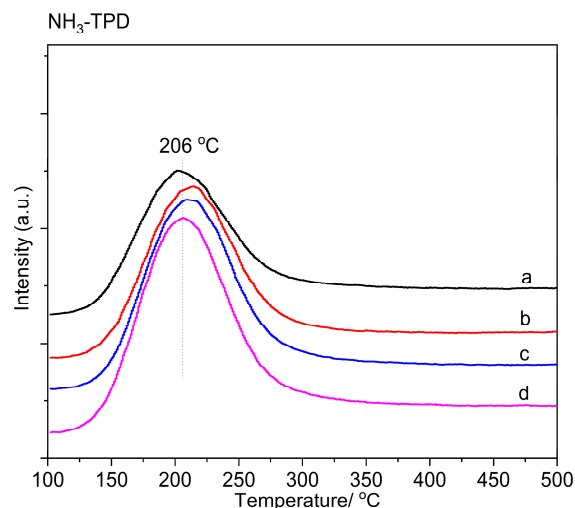


Figure 4. NH_3 -TPD spectra of zeolites: (a) CsX_37; (b) CsX_31; (c) CsX_24; and (d) CsX_10.

Figure 5 presents the CO_2 -TPD characterization results of the four CsX zeolites. All four CsX zeolites exhibit a CO_2 desorption peak at approximately 194.8 °C, indicating the presence of medium-strength alkali centers on their surfaces. The intensity of these alkali centers shows minimal variations across the zeolites. The order of CO_2 desorption is $\text{CsX}_{37} > \text{CsX}_{31} > \text{CsX}_{24} > \text{CsX}_{10}$. These findings suggest that as the Cs content in CsX increases, the strength of the alkali centers remains relatively constant and the number of alkali centers gradually increases. Specifically, the Cs^+ ion in the zeolite cage interacts with the surrounding skeleton oxygen, resulting in a reduced shielding effect of the metal cations on the oxygen electrons of the zeolite skeleton. Consequently, the electron-donating ability of the skeleton oxygen is enhanced, thereby increasing the level of alkalinity. Additionally, the O in Cs_2O can function as a basic center, and the Cs^+ ion in the zeolite cage can serve as a Lewis acid center. Notably, Cs_2O exhibits high reactivity and can react with CO_2 and H_2O in the air when exposed for extended periods of time, leading to a decrease in the alkalinity of the zeolite. However, roasting the catalyst at a high temperature (600 °C) under an air atmosphere can effectively restore its alkalinity.

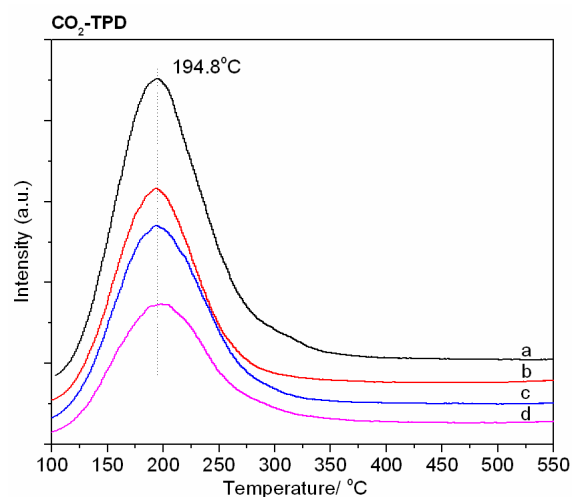


Figure 5. CO_2 -TPD profiles of zeolites: (a) CsX_37; (b) CsX_31; (c) CsX_24; and (d) CsX_10.

2.1.5. States of Cs Species and Oxygen Species

To investigate the chemical nature of cesium species on the surface and in the inner sections of CsX, Figures 6 and 7 present the XPS spectra in the Cs 3d_{5/2} and O 1s regions for both samples, respectively. All samples exhibited two peaks, suggesting the presence of cesium in two chemical states. The Cs 3d_{5/2} peak at 724.5 eV corresponds to the exchange cation Cs⁺, while the peak at 725.0~725.2 eV is attributed to the Cs₂O phase [18]. As observed in the order of CsX_10, CsX_24, and CsX_31, the content of Cs⁺ ions on the molecular sieve's surface and at a depth of 50 nm gradually increased (Table 3). Moreover, the characteristic peaks of Cs⁺ ions on the surface and inside CsX_31 became more pronounced, indicating a change in the form of cesium species with the increasing degree of Cs ion exchange. The concentration of Cs⁺ ions in CsX_31 is higher than that of Cs₂O, whereas the concentration of Cs₂O in the other two types of CsX is higher than that of Cs⁺ ions.

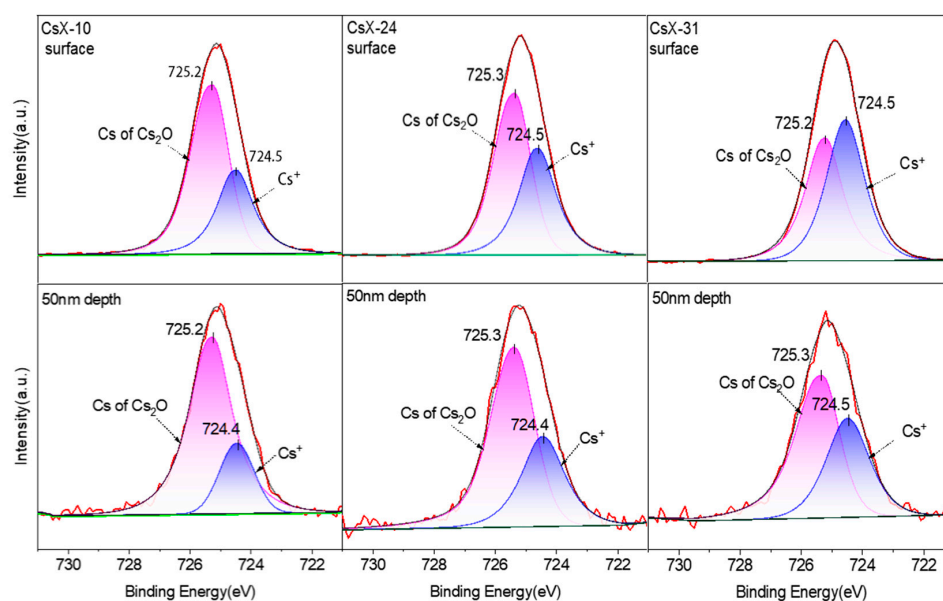


Figure 6. Cs 3d_{5/2} spectra in different depths of CsX_10, CsX_24, and CsX_31.

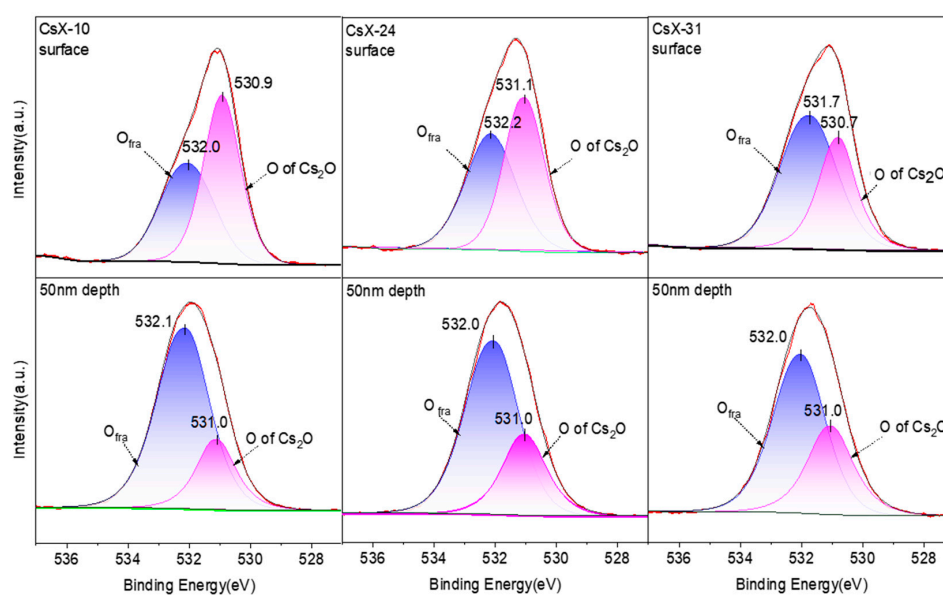


Figure 7. O 1s spectra in different depths of CsX_10, CsX_24, and CsX_31.

Table 3. Cs 3d_{5/2} and O 1s XPS analyses of CsX_n catalysts.

XPS Spectra		Cs 3d _{5/2}		O 1s	
Binding Energy (eV)		724.4	725.2	531.7–532.2	530.9
Assignment		Cs of Cs ⁺	Cs of Cs ₂ O	O of Framework	O of Cs ₂ O
Catalyst	Depth	ηCs _{ion} (%)	ηCs _{oxi} (%)	ηO _{fra} (%)	ηO _{oxi} (%)
CsX-10	Surface	33.11	66.89	44.84	55.16
	50 nm	17.94	78.52	76.75	23.25
CsX-24	Surface	41.08	58.92	48.50	51.50
	50 nm	33.33	66.67	70.91	29.09
CsX-31	Surface	52.29	47.71	62.62	37.38
	50 nm	39.17	60.83	66.04	33.96

At a depth of 50 nm, the total Cs content is lower than that of the surface. The content of Cs⁺ ions is notably lower than that of Cs₂O. As the degree of Cs ion exchange increases, Cs⁺ content shows an upward trend while Cs₂O content shows the opposite. This depth aligns with the Cs₂O grain size calculated from the XRD results, suggesting that the particle surface of CsX molecular sieve X is covered with a 50 nm layer of Cs₂O. During side chain alkylation, Cs⁺ species can adsorb and activate toluene as a Lewis acid, altering the basicity of the oxygen backbone. Simultaneously, Cs₂O species offer stronger basic sites, enhancing methanol's dehydrogenation into formaldehyde. However, excessive Cs₂O (overly strong basic sites) may accelerate methanol's deep decomposition into CO and H₂.

When analyzing the material from the CsX's surface up to a depth of 50 nm, two different characteristic peak positions are observed for its O 1s binding energies (BEs). The O 1s signal at 530.9 eV corresponds to the oxygen atoms of the Cs₂O crystal phase, while the O 1s signal ranging from 531.7 to 532.2 eV is attributed to the oxygen framework. Table 3 provides a summary of the XPS-based quantitative analysis results for cesium and oxygen in the CsX catalyst. The O 1s spectrum analysis reveals that the framework oxygen content on the CsX surface gradually increases with the degree of Cs ion exchange. Interestingly, a significant increase in the framework oxygen content of CsX is observed when analyzing species at a depth of 50 nm. This suggests that the particle surface of CsX molecular sieve X is covered with a layer of the Cs₂O phase, consistent with the Cs 3d_{5/2} spectral analysis results. The majority of oxygen below the 50 nm surface is attributed to framework oxygen, while the remaining oxygen is likely associated with the highly dispersed Cs₂O phase found in the inner cavities or pores of the X molecular sieve crystals. The O 1s BE of zeolite is correlated with the alkalinity of the framework oxygen, with its higher alkaline strength corresponding to lower O 1s BE values [18]. Notably, the O 1s BE peak positions in CsX are all approximately 530.9 eV, indicating a similar alkaline strength across different ion exchanges in CsX. This observation aligns with the CO₂-TPD results.

2.2. Adsorption and Activation Properties of Methanol on CsX

2.2.1. Adsorption of Methanol on CsX (In Situ Infrared Characterization)

The adsorption properties of CsX₃₁ for methanol were investigated by employing in situ FT-IR measurements. Figure 8 presents the in situ infrared absorption spectra of methanol on various CsX samples evacuated at 140 °C. Similar to CsX₃₁, CsX₃₇ also exhibits peaks at 1692 and 1290 cm⁻¹. However, the intensities of these peaks are lower, suggesting that CsX₃₇ has a weaker ability to adsorb formaldehyde than CsX₃₁. The C=O absorption peaks corresponding to the formaldehyde species on the surfaces of the CsX₂₄ and CsX₁₀ zeolites are observed at 1692 cm⁻¹ and 1688 cm⁻¹, respectively. Notably, the peak intensity of CsX₂₄ is higher than that of CsX₁₀. Furthermore, the peak intensity at 1290 cm⁻¹ changes. Notably, the peak intensity of CsX₁₀ is the weakest among the observed changes. The peaks of the CsX₃₇, CsX₂₄, and CsX₁₀ zeolites at 1381 cm⁻¹, which correspond to the CO stretching vibration peak in monodentate formate, shift slightly towards higher wave numbers (CsX₃₁: 1383 cm⁻¹). This indicates that the C–O bond

is enhanced in monodentate formate. No characteristic peaks of bidentate formate (1609 and 1338 cm^{-1}) are observed on the surfaces of CsX_37, CsX_24, and CsX_10. In NaX, only a minor amount of formaldehyde absorption peaks is observed, with no distinctive peaks indicating the presence of monodentate or bidentate formate. These results indicate that various CsX catalysts exhibit distinct abilities in adsorbing and activating methanol. Moreover, the quantity of formaldehyde intermediates generated on the catalyst's surface and the capacity to form formate vary. The adsorption and activation of methanol on CsX_24 and CsX_10 are low, resulting in the generation of small amounts of active intermediates (formaldehyde and monodentate formate). The ability of CsX_37 to activate methanol is excessively strong, leading to further decomposition of the generated active intermediates into CO_2 and H_2 . This decomposition occurs because of the breakdown of bidentate formate [23]. CsX_31 exhibits moderate methanol adsorption and activation capabilities. The catalyst's surface effectively adsorbs formaldehyde and monodentate and bidentate formate.

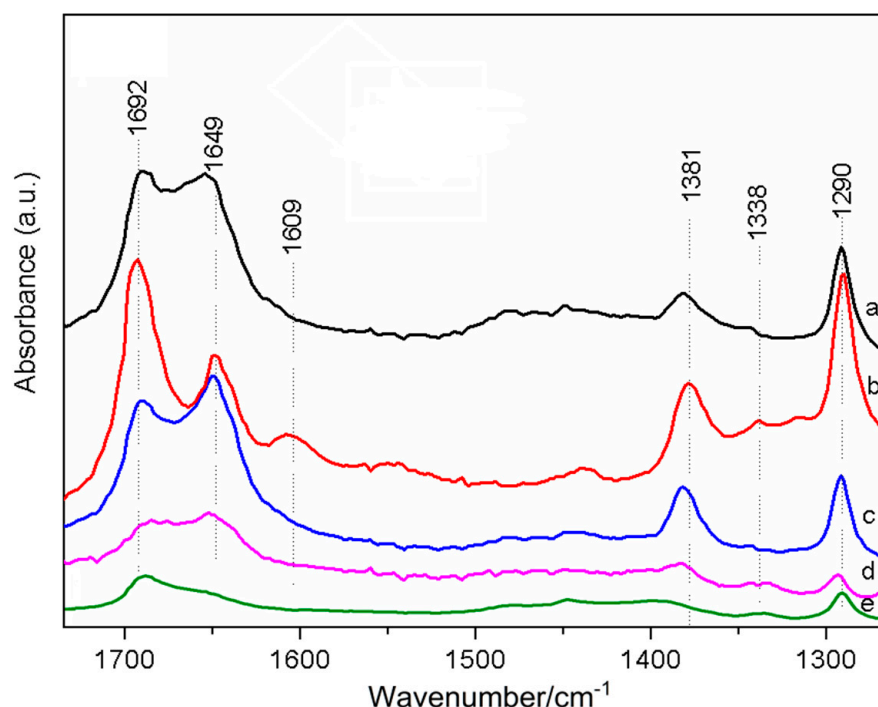


Figure 8. FT-IR spectra of methanol on desorbed CsX. Methanol pre-adsorbed on CsX at $50\text{ }^{\circ}\text{C}$ and then evacuated at $140\text{ }^{\circ}\text{C}$: (a) CsX_37; (b) CsX_31; (c) CsX_24; (d) CsX_10; and (e) NaX.

2.2.2. Decomposition of Methanol on CsX (TPD-MS Analysis)

To gain a deeper understanding of the adsorption and activation of methanol on CsX, the decomposition products of methanol on CsX were analyzed by performing quadrupole MS. Figure 9 shows that methanol decomposes on all CsX samples, resulting in the production of CO , H_2 , HCHO , CO_2 , and CH_4 as the main decomposition products. Specifically, CH_3OH decomposes to produce H_2 and HCHO [8,24]. HCHO is unstable and readily converted into formate species. Monodentate formate decomposes to generate CO and H_2O , whereas bidentate formate decomposes to generate CO_2 and H_2 [23]. CH_4 is generated through the following reaction [22]:



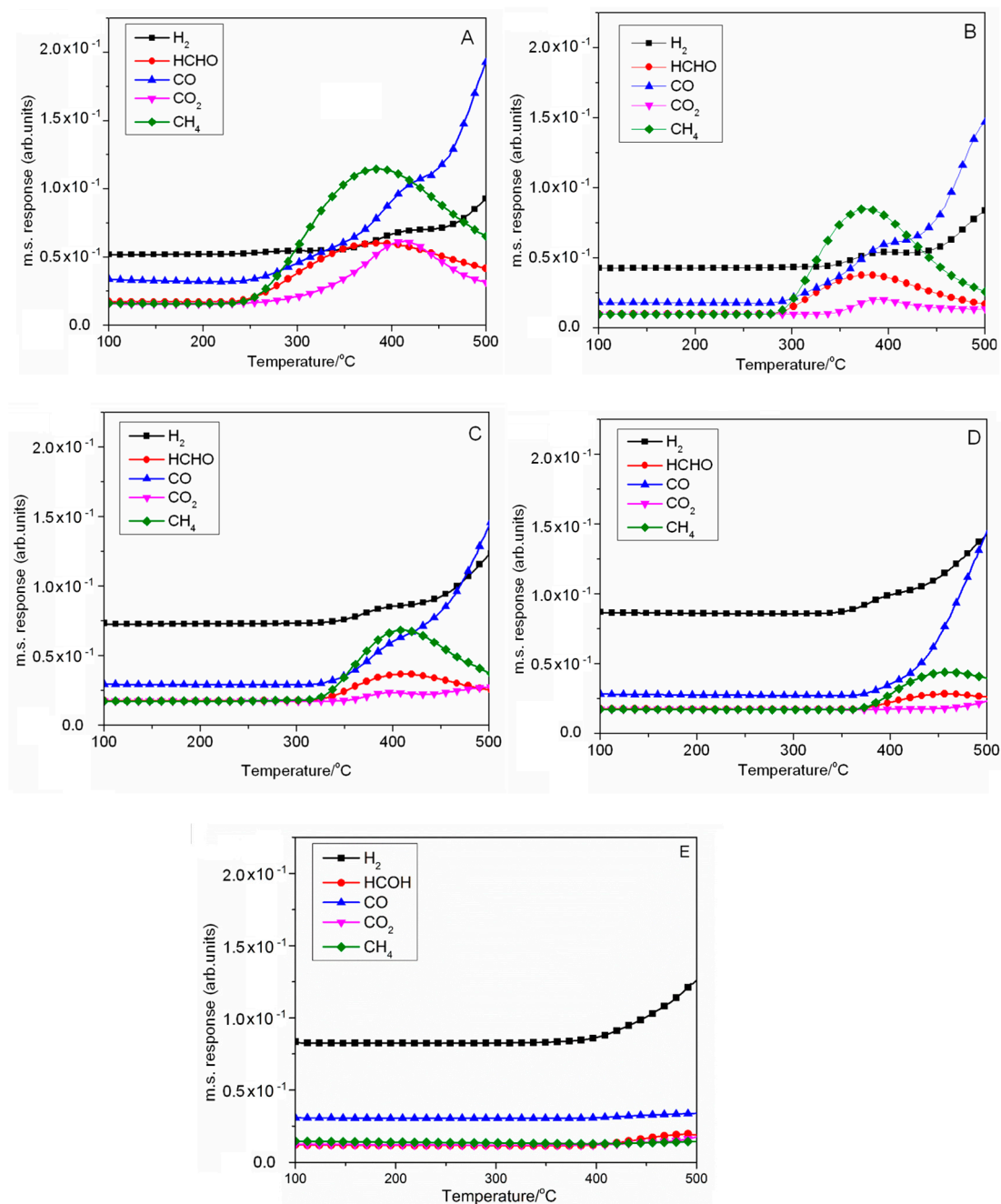
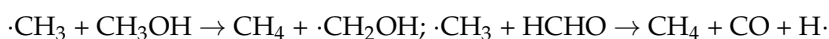


Figure 9. TPD decomposition of methanol over CsX: (A) CsX_37; (B) CsX_31; (C) CsX_24; (D) CsX_10; and (E) NaX.

Chen et al. [25] investigated the side chain alkylation radical mechanisms of toluene and methanol. They discovered that methanol can potentially undergo the following side chain reactions, resulting in the formation of CH_4 :



As shown in Figure 9A, methanol on CsX_37 starts decomposing at 242 °C, resulting in the formation of H_2 , CO, HCHO, and CH_4 as the decomposition products. As the temperature increases, the amounts of desorbed H_2 and CO gradually increase, displaying similar trends. The desorption amounts of CO_2 , HCHO, and CH_4 initially increase and then decrease with an increasing temperature and reach their maximum values at 389, 389,

and 417 °C, respectively. Additionally, the desorption amount of CO shows a significant increase starting at 417 °C, indicating that high temperatures promote CO generation. These results demonstrate the strong decomposition ability of methanol on CsX₃₇. The formaldehyde produced from methanol decomposition undergoes further conversion into formate species, which subsequently decompose into CO, H₂O, CO₂, and H₂, resulting in the generation of more CH₄.

The decomposition temperature of methanol on CsX₃₁ is approximately 278 °C, as shown in Figure 9B. The main products of this decomposition are CO, CH₄, HCHO, and H₂. CO₂ starts to be generated at 347 °C, and its desorption gradually increases with the temperature, reaching a maximum at approximately 400 °C. Figure 9C reveals that methanol on CsX₂₄ begins to decompose at 305 °C. The resultant products are primarily CO, CH₄, HCHO, and H₂. CO₂ starts to be generated at 350 °C, and its desorption increases slowly with the temperature, reaching a maximum at approximately 400 °C (with a small range of change). Figure 9D illustrates that methanol exhibits minimal reactivity towards CsX₁₀ at low temperatures. Methanol starts decomposing at 367 °C, resulting in the formation of CH₄, CO, H₂, and HCHO, with negligible production of CO₂. As the temperature increases to 459 °C, a small amount of CO₂ is observed, indicating that CsX₁₀ possesses a limited capacity for methanol decomposition and can catalyze methanol decomposition at elevated temperatures. Figure 9E demonstrates that NaX exhibits the lowest methanolysis performance. At temperatures exceeding 400 °C, the generation of H₂ is observed, along with a small quantity of HCHO. However, with a further temperature increase, only trace amounts of CH₄, CO, and CO₂ are detected.

Compared with those on CsX₃₇, the decomposition products of methanol on the other CsX materials are essentially identical, and the desorption amounts of all products exhibit similar trends as the temperature increases. However, the initiation temperature for methanol decomposition varies among CsX materials with different Cs contents. When the Cs content in CsX is low, the temperature at which methanol begins to decompose is high. As the Cs content increases, the temperature at which methanol begins to decompose gradually decreases. Simultaneously, the amount of almost every product gradually increases. In comparison to NaX, CsX exhibited increased production of products (CO and CO₂) resulting from the excessive decomposition of methanol. This phenomenon can be attributed to the gradual increase in the number of basic centers with an increasing Cs content.

2.3. The Effect of the Ion Exchange Temperature on Catalytic Performance

The impact of the ion exchange temperature on the catalyst's performance was examined, and the results are presented in Table 4. The Cs content increases as the exchange temperature increases. A higher exchange temperature promotes the exchange of Cs ions, and increasing the number of ion exchanges benefits the exchange of Cs ions. The performances of the catalysts also show significant differences. As the Cs content increases, the toluene conversion rate and total yield of side chain alkylation increase. However, a sharp decline in catalytic activity is observed when the Cs content reaches 37.8 wt%. The reaction is primarily driven by the side chain alkylation of toluene, resulting in the generation of only a small amount of benzene ring alkylation products. The total selectivity for side chain alkylation on all CsX catalysts is greater than 95%. Furthermore, this total selectivity does not significantly change with an increasing Cs content. The highest toluene conversion rate (6.5%) and total yield of side chain alkylation (6.4%) are achieved when the Cs content is 31.8 wt%. Methanol utilization initially increases and then decreases as the Cs content increases. The maximum methanol utilization of 19.2% is observed when the Cs content is 31.8 wt%. Notably, the methanol conversion rates on all CsX catalysts are greater than 98%, which suggests that methanol undergoes excessive decomposition on these catalysts at a reaction temperature of 435 °C. Upon exposure to air, the reactivity of the CsX catalyst notably diminishes over time in comparison to its freshly prepared state. This decline in reactivity is linked to the existence of alkaline centers, like Cs₂O, on the

catalyst's surface. When the catalyst is exposed to air during the placement process, these alkaline centers react with H₂O and CO₂, leading to the formation of cesium carbonate-like or cesium bicarbonate species. The formation of these species ultimately results in a decline in catalytic activity. However, high-temperature calcination (600 °C) can restore the activity of CsX catalysts that have been left for a certain effluxion of time.

Table 4. The effect of temperature on the catalytic performance of CsX catalysts ¹ in the side chain alkylation reactions of toluene and methanol.

Catalyst	Temperature of Ion Exchange/°C	Cs Content /wt%	C _{Tol} ⁵	S _{St} ⁵	S _{others} ²	S _{St+E} ⁵	Y _{St} ⁵	Y _{St+E} ⁵	U _{Me} ⁵
CsX_10 ³	60	10.1	2.0	63.7	4.7	95.3	1.3	1.9	7.2
CsX_14 ³	70	14.2	2.5	58.0	4.9	95.1	1.4	2.3	8.1
CsX_18 ³	90	18.2	3.0	55.5	2.0	98.0	1.7	3.0	10.4
CsX_24 ⁴	60	24.0	4.6	24.2	2.3	97.7	1.1	4.5	14.2
CsX_31 ⁴	70	31.8	6.5	20.6	2.1	97.9	1.3	6.4	19.2
CsX_34 ⁴	80	34.2	6.3	22.9	2.3	97.7	1.4	6.2	18.9
CsX_37 ⁴	90	37.8	2.3	31.8	1.7	98.3	0.7	2.3	7.4

¹ Reaction conditions: WHSV of 2.0 h⁻¹, toluene/methanol ratio of 3/1, reaction temperature of 435 °C, and reaction time of 2 h. ² Other byproducts include xylenes, trimethylbenzene, and benzene. ³ The ion exchange occurred once. ⁴ The ion exchange occurred twice. ⁵ C: conversion (%); S: selectivity (%); Y: yield (%); U: utilization (%); Tol: toluene; me: methanol; St: styrene; and St+E: styrene and ethylbenzene.

All the catalysts exhibited a high degree of methanol conversion (>95%). However, the utilization efficiency of methanol shows a trend of first increasing and then decreasing with the increase in Cs content. This could be because the strong basic sites that are active for the side chain alkylation reactions of toluene and methanol also catalyze the undesired methanol decomposition reaction at roughly 10 times the rate [13]. It is commonly accepted in the literature that an excess of Cs₂O (a strongly basic site) may lead to the deep decomposition of methanol into CO [7,18–20].

2.4. Properties of Active Centers in CsX Catalysts

The nature of the active center of the catalyst and its role in the side chain alkylation reaction of toluene have been extensively studied [21,26–28]. The alkylation of toluene and methanol proceeds smoothly through the synergistic effect of the acid–base center [29,30]. The basic center plays a crucial role in this process.

A sufficiently strong basic center can facilitate the dehydrogenation of toluene, resulting in the formation of alkylating reagents such as formaldehyde and formate [31]. Additionally, the basic center can activate the methyl group present in the toluene side chain. The appropriate acidic centers on the catalyst are mainly used to stabilize the adsorption of activated toluene. When the acidic centers on the zeolite surface and the pores are in close proximity, the activated toluene adsorbed by the acidic centers can effectively come into contact with the alkylating reagent (formaldehyde or formate), leading to the side chain alkylation reaction. However, the reaction process and the active center of this reaction are still not fully understood. Therefore, further research is required to determine the effect of the Cs content on the properties of the active centers of NaX zeolites and the activity of these catalysts in the alkylation reactions between toluene and methanol during Cs ion modifications.

The relevant literature and the results of NH₃-TPD, CO₂-TPD, and the BET surface area that the CsX catalyst prepared by using CsNO₃ as the cesium source primarily consist of Cs species in three different states. Cesium is found in the form of Cs ions within the zeolite cage, which leads to a reduction in S_{BET} but improves the stable adsorption of active intermediates (e.g., monodentate formate). Additionally, Cs⁺ ions interact with specific defective sites in the zeolite framework, resulting in the formation of cesium silicate-like species or slight modifications in the zeolite's structure. Moreover, Cs is well-dispersed on the zeolite's surface as Cs₂O, blocking some pores and increasing the strength and quantity

of alkaline centers. However, an excess of strong basic centers may lead to excessive methanol decomposition.

The zeolite cage undergoes electrostatic interactions with the Cs ions and surrounding oxygen skeleton. The large radius of the Cs ions reduces the shielding effect on the oxygen electrons of the zeolite skeleton, thereby enhancing the electron-donating ability of the skeleton oxygen (known as alkali sexual enhancement). This basic center can be used as an active center for the activation of toluene and methanol. Additionally, the O in Cs₂O can serve as a basic center for activating toluene and methanol. Cs ions located at the SII and SIII positions within the zeolite cage (Figure 10) can be stably adsorbed as Lewis acid centers, which can activate toluene and the reactive intermediates produced from methanol. Increasing the temperature and number of ion exchanges can enhance the Cs content in CsX. With an increase in Cs loading amount, the strength of the basic centers of CsX remains stable, whereas the number of basic centers significantly increases. However, the strength and number of acidic centers in the catalyst remain largely unchanged. The CO₂-TPD results suggest that the strengths of the two alkali centers are similar.

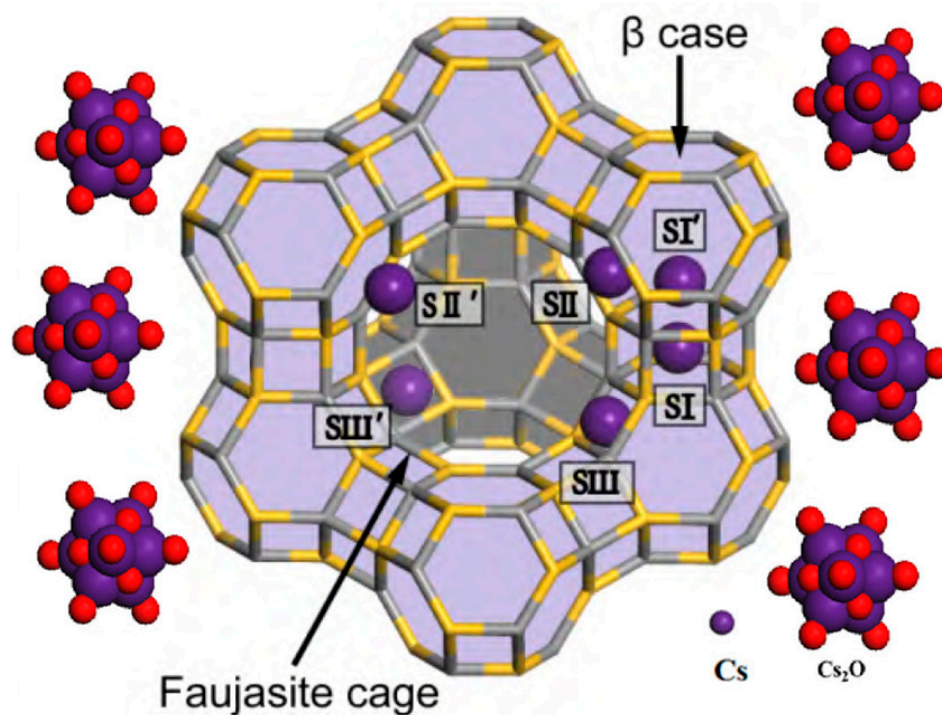


Figure 10. Topology structure of faujasite zeolite and its three cations sites (SI, SII, and SIII) [25].

When the Cs content is 10.1 wt%, both the toluene conversion rate and methanol utilization rate on the catalyst are low, and methanol is almost completely converted. This result suggests that the Cs ions in the CsX₁₀ zeolite cage can function as Lewis acid centers and effectively adsorb toluene. However, the number of basic centers is limited, resulting in a low probability of benzyl activation. Consequently, the basic centers activate methanol, generating formaldehyde and monodentate formate as active intermediates. Additionally, the small amount of Cs ions leads to a reduced number of active intermediates that can be stably adsorbed by the Lewis acid centers. This is evident from the weak characteristic absorption peak intensities of formaldehyde and the monodentate formate acidic salt in the in situ infrared spectrum of CsX₁₀. The probability of reactive intermediates being generated from the reaction between methanol and activated toluene is ultimately reduced. Consequently, most of these intermediates undergo further decomposition into carbon monoxide (CO) and hydrogen (H₂). This phenomenon is observed in the TPD-MS analysis, where CsX₁₀ produces a high amount of CO at 435 °C. Moreover, the concentration of Cs⁺ ions in the β cage of CsX₁₀ is low, which makes it more susceptible to side reactions with

methanol [25]. The activation of toluene on CsX_10 is crucial for facilitating the side chain alkylation of toluene. When the Cs content is 10.1–34.2 wt%, both the toluene conversion rate and methanol utilization rate gradually increase with an increasing Cs content. This phenomenon can be attributed to the increase in the Cs content, which leads to an increase in the numbers of the two types of basic centers on CsX. Consequently, the activation probability of toluene increases. Additionally, the high content of Cs⁺ ions located in the β cage stabilizes it through the Lewis acid center. The increase in the amount of adsorbed active intermediates (as observed in the in situ infrared spectrum, where the intensities of the characteristic absorption peaks of formaldehyde and monodentate formate gradually increase with an increasing Cs content) enhances the likelihood of side chain alkylation reactions. Furthermore, the high amount of Cs⁺ ions entering the β cage effectively impedes the progression of methanol side reactions, thereby improving methanol utilization.

When the concentration of Cs in the CsX catalyst is increased to 37.8 wt%, numerous basic centers are present. Consequently, some of the Cs₂O obstructs the pores of the zeolite, hindering the entry of toluene into the supercage. Simultaneously, the abundance of basic centers promotes methanol production. The presence of excess basic centers can lead to side reactions, producing CH₄, CO, and CO₂ before the activated toluene can react. This is evident from the weakening of the characteristic absorption peaks of formaldehyde and monodentate formate in the in situ infrared spectrum of CsX_37, as well as from the significantly higher amounts of CH₄, CO, and H₂ detected in the MS analysis of CsX_37 compared with those of the other catalysts. Methanol activation plays a crucial role in side chain alkylation reactions. For the effective activation and decomposition of methanol, an appropriate number of basic centers that match the properties of the acid–base centers on CsX are necessary. This allows CsX to moderately activate and decompose methanol, leading to the formation of stable active intermediates such as formaldehyde and monodentate formate. Additionally, sufficient basic centers are important for the activation of toluene, and the activated toluene adsorbed on adjacent active centers can undergo side chain alkylation reactions with formaldehyde or monodentate formate. This ultimately improves methanol utilization and promotes toluene conversion.

3. Discussion

Previous studies have revealed that high-performance side chain alkylation catalysts typically possess the following characteristics: (1) a sufficiently strong basic center should be present to facilitate the dehydrogenation of methanol, leading to the formation of formaldehyde, which serves as a bona fide alkylation reagent. Additionally, the catalysts should activate the benzyl groups in toluene. (2) Sufficient acidic centers should be available for the stable adsorption of activated toluene. Additionally, the acid and alkali centers must be in close proximity on the surface and pores of the zeolite. This proximity facilitates contact between the generated alkylating reagent and activated toluene, thereby enabling side chain alkylation reactions [28]. Early works also suggested that the presence of a high density of basic sites in the CsX catalyst is related to the transformation of unidentate formate into bidentate formate, an unfavorable intermediate that can be easily transferred to CO and H₂, thus decreasing the utilization of methanol and side chain product yield [32].

In this study, several CsX catalysts were prepared using the ion exchange method with different numbers of ion exchanges and exchange temperatures. Various characterization results confirmed that increasing the number of ion exchanges and the exchange temperature effectively increased the Cs content. A portion of the introduced Cs species was present in the zeolite cage as Cs⁺ ions, which serve as Lewis acid centers for the stable adsorption of toluene and alkylation reagents (e.g., formaldehyde or monodentate formate). The alkalinity of skeletal oxygen in the zeolite cage increased because it served as an active center for the activation of toluene and methanol. Some Cs species were highly dispersed on the surface of the zeolite in the form of Cs₂O. The O in Cs₂O also acted as an alkaline center for the activation of toluene and methanol. As the Cs content increased, the number of basic centers in the catalyst gradually increased, and the base's strength remained unchanged.

Additionally, some acidic centers existed in the catalyst, and changes in the Cs content had a minimal impact on the properties of these acidic centers on the catalyst's surface. All the CsX zeolite catalysts exhibited catalytic activity and high selectivity (>95%) for the side chain alkylation of toluene and methanol. The toluene conversion rate considerably varied with changes in the preparation parameters. Specifically, as the Cs content increased, the toluene conversion rate gradually increased. At a Cs content of 34.2 wt%, the toluene conversion rate was at its highest (6.5% at 435 °C). However, a further increase in the Cs content led to a reduction in the toluene conversion rate.

A combination of in situ infrared characterization and MS analysis revealed that the activity of the toluene side chain alkylation reaction on the CsX catalyst was determined by the nature of the basic center. The catalyst's ability to activate methanol and toluene gradually increased with an increasing number of basic centers. However, when the Cs content was low, the catalyst's surface contained a small number of alkaline centers, resulting in a low amount of activated toluene. Consequently, the probability of the occurrence of a side chain reaction with the active intermediate generated through methanol decomposition was low, leading to low reaction activities. When the concentration of Cs was extremely high, an excessive number of alkali centers caused the formaldehyde and formate intermediates, which were produced through methanol activation, to decompose rapidly into CH₄, CO, CO₂, H₂, and other byproducts before they had sufficient time to react with the activated toluene. This resulted in reduced methanol utilization and a decrease in the reaction rate, which subsequently reduced the toluene conversion rate. The catalyst's ability to activate and decompose methanol was moderate when the number of basic centers was appropriate. This led to the generation of active intermediates, such as formaldehyde and monodentate formate, which were stable and easily adsorbed on adjacent active centers. The side chain alkylation of toluene in the solvent enhanced the methanol utilization rate, thereby promoting toluene conversion.

4. Materials and Methods

4.1. Catalyst Preparation

A series of CsX catalysts were prepared by the ion exchange of NaX (Si/Al = 1.3). The detailed preparation steps are as follows: NaX (0.6 g) was treated at temperatures ranging from 60 to 90 °C for 2 h in a 0.2 mol/mL aqueous solution of cesium salts. The resulting sample was then filtered and washed with an excess of deionized water. The obtained materials were dried overnight at 100 °C and subsequently calcined in air at 600 °C for 4 h. Some samples underwent this procedure once more for repetition.

4.2. Catalytic Experiments

The methylation of toluene with methanol was conducted in a vertical, fixed-bed quartz reactor under atmospheric pressure. Prior to this experiment, all samples were pressed, crushed, and sieved to obtain particles of size 40–60 mesh. Following this, 0.5 g of the catalyst was loaded onto the reaction bed and activated at 450 °C for 2 h under an air atmosphere. The aim of this pretreatment was to eliminate any water and carbon dioxide that may have been adsorbed on the catalyst's surface. The catalysts obtained were labeled as CsX₁₀, CsX₁₄, CsX₁₈, CsX₂₄, CsX₃₁, CsX₃₄, and CsX₃₇, with the number indicating the weight percentage of Cs content.

Lowering the reaction temperature, we switched the carrier gas to inert gas nitrogen and utilized a micro-injection pump to introduce the reactants from the upper end of the reactor. The mass space hourly velocity of the reactants varied from 1 to 6 h⁻¹. The different gaseous products were analyzed by a 3420A gas chromatograph from Beifen Ruili Company (Beijing, China). The capillary chromatography column model was FFAP. Additionally, we employed a hydrogen flame ion detector as the detector and high-purity nitrogen as the carrier gas. The detection room temperature was maintained at 280 °C, while the gasification chamber temperature was set at 260 °C.

4.3. Catalyst Characterization

Powder XRD patterns were recorded using a Shimadzu XRD-6000 X-ray diffractometer (Kyoto, Japan) equipped with Cu K α radiation ($\lambda = 1.4518 \text{ \AA}$). The X-ray tube was operated at 40 kV and 30 mA. The spectra were recorded from 4° to 40°. The spectrogram of Fourier-transform infrared spectroscopy was measured using the Nicolet™ 6700 infrared spectrometer (Thermo Scientific, Waltham, MA, USA). Support plates were used for testing, and the wave number range recorded in the infrared spectrum was within 1200–3800 cm^{-1} . The experimental conditions for the pyridine adsorption infrared analysis were as follows: The support plates were treated at 300 °C under vacuum (10^{-4} mmHg) for 30 min in an in situ IR cell. After cooling to room temperature, pyridine was adsorbed for 30 min. The sample cell was then evacuated to 10^{-4} mmHg at room temperature using a vacuum pump (Thermo Scientific, Waltham, MA, USA). Subsequently, the temperature was raised to 150 °C, and the vacuum was maintained for 30 min. Finally, the sample was cooled back to room temperature for infrared testing. N₂ adsorption–desorption isotherms were obtained using a Micromeritics ASAP 2010N physical adsorption analyzer system at –196 °C (Norcross, GA, USA). Prior to testing, the samples were treated at 250 °C under vacuum conditions for 12 h. The specific surface area was determined using the BET formula, and the pore size distribution was calculated using the BJH model. NH₃-TPD (temperature-programmed desorption) and CO₂-TPD experiments were conducted on a TP-5079 fully automatic multi-purpose adsorption instrument device (Tianjin Xianquan, Tianjin, China). The desorbed NH₃ was detected using gas chromatography with a thermal conductivity detector (TCD) (Thermo Scientific, Waltham, MA, USA). The same procedure was followed for the CO₂-TPD experiments, except that pure carbon dioxide was used as the absorption gas. The sample, with a particle size of 40–60 mesh, was treated within a temperature range of 400 to 500 °C for 1 h under high-purity helium gas flow (20 mL/min). Afterward, the sample was cooled to 100 °C and purged with high-purity helium for 30 min to remove physically adsorbed NH₃ molecules. Subsequently, desorption data were recorded using a thermal conductivity detector (TCD). Scanning electron microscopy (SEM) images and energy-dispersive X-ray spectroscopy (EDS) maps were obtained using a Hitachi X-65 instrument (Tokyo, Japan) operating under an acceleration voltage of 10 kV. Our aim was to identify and document the morphological characteristics, particle size distribution, and elemental energy distribution of the material under investigation. The AXIOS X-ray fluorescent spectrometer (Malvern Panalytical, Malvern, UK) was used in X-ray fluorescence spectroscopy. It was designed to measure the mass percentage of each element present in the material being tested.

5. Conclusions

In the present study, several CsX catalysts were prepared using the ion exchange method with different numbers of ion exchanges and exchange temperatures. A variety of characterization results, including FT-IR and TPD, confirmed that increasing the number of ion exchanges and exchange temperature effectively increased the Cs content. A portion of the introduced Cs species was present in the zeolite cage as Cs⁺ ions, which serve as Lewis acid centers for the stable adsorption of toluene and alkylation reagents (e.g., formaldehyde or monodentate formate). A combination of in situ infrared characterization and MS analyses revealed that the activity of the toluene side chain alkylation reaction on the CsX catalyst was determined by the nature of the basic center. The catalyst's ability to activate and decompose methanol was moderate when the number of basic centers was appropriate. This led to the generation of active intermediates, such as formaldehyde and monodentate formates, which were stable and easily adsorbed onto adjacent active centers. The side chain alkylation of toluene in the solvent enhanced the methanol utilization rate, thereby promoting toluene conversion.

Author Contributions: Z.Z. conceptualization, data curation, formal analysis, investigation, methodology, software, visualization, writing—original draft, writing—review and editing, validation. Q.W.: software, data curation, methodology, writing—original draft, validation. W.G.: formal analysis, investigation, writing—original draft, validation. C.M.: software, visualization, validation. M.Y.: software, validation, data curation. All authors have read and agreed to the published version of the manuscript.

Funding: The authors greatly appreciate the financial support by the Jilin Provincial Science and Technology Development Plan Project (No. 222621JC010299261), the Jilin Provincial Department of Education Science and Technology Research Project (No. JJKH20230286KJ), and the Jilin Institute of Chemical Technology Doctoral Start-up Fund (No. 2020004).

Data Availability Statement: All data generated or analyzed during this study are included in this published article.

Conflicts of Interest: Author Chunxiang Ma was employed by the Research Institute of PetroChina Jilin Petrochemical Company. The remaining authors declare that the research was conducted in the absence of any commercial or financial relationships that could be construed as a potential conflict of interest.

References

1. Kovacevic, M.; Agarwal, S.; Mojet, B.L.; Ommen, J.G.V.; Lefferts, L. The effects of morphology of cerium oxide catalysts for dehydrogenation of ethylbenzene to styrene. *Appl. Catal. A Gen.* **2015**, *505*, 354–364. [[CrossRef](#)]
2. Jin, M.; Feng, X.; Feng, L.; Sun, T.; Zhai, J.; Li, T.; Jiang, L. Superhydrophobic Aligned Polystyrene Nanotube Films with High Adhesive Force. *Adv. Mater.* **2005**, *17*, 1977–1981. [[CrossRef](#)]
3. Arrighi, V.; McEwen, I.J.; Qian, H.; Serrano Prieto, M.B. The glass transition and interfacial layer in styrene-butadiene rubber containing silica nanofiller. *Polymer* **2003**, *44*, 6259–6266. [[CrossRef](#)]
4. Meincke, O.; Kaempfer, D.; Weickmann, H.; Friedrich, C.; Vathauer, M.; Warth, H. Mechanical properties and electrical conductivity of carbon-nanotube filled polyamide-6 and its blends with acrylonitrile/butadiene/styrene. *Polymer* **2004**, *45*, 739–748. [[CrossRef](#)]
5. Borgna, A.; Magni, S.; Sepulveda, J.; Padro, C.L.; Apesteguia, C.R. Side-chain alkylation of toluene with methanol on Cs-exchanged NaY zeolites: Effect of Cs loading. *Catal. Lett.* **2005**, *102*, 15–21. [[CrossRef](#)]
6. Song, L.; Li, Z.; Zhang, R.; Zhao, L.; Li, W. Alkylation of toluene with methanol: The effect of K exchange degree on the direction to ring or side-chain alkylation. *Catal. Commun.* **2012**, *19*, 90–95. [[CrossRef](#)]
7. Han, H.; Liu, M.; Ding, F.; Wang, Y.; Guo, X.; Song, C. Effects of Cesium Ions and Cesium Oxide in Side-Chain Alkylation of Toluene with Methanol over Cesium-Modified Zeolite X. *Ind. Eng. Chem. Res.* **2016**, *55*, 1849–1858. [[CrossRef](#)]
8. Hunger, M.; Schenk, U.; Weitkamp, J. Mechanistic studies of the side-chain alkylation of toluene with methanol on basic zeolites Y by multi-nuclear NMR spectroscopy. Dedicated to Professor Herman van Bekkum on the occasion of his 65th birthday 1. *J. Mol. Catal. A Chem.* **1998**, *134*, 97–109. [[CrossRef](#)]
9. Alabi, W.O.; Tope, B.B.; Jermy, R.B.; Aitani, A.M.; Hattori, H.; Al-Khattaf, S.S. Modification of Cs-X for styrene production by side-chain alkylation of toluene with methanol. *Catal. Today* **2014**, *226*, 117–123. [[CrossRef](#)]
10. Palomares, A.E.; Eder-Mirth, G.; Rep, M.; Lercher, J.A. Alkylation of Toluene over Basic Catalysts—Key Requirements for Side Chain Alkylation. *J. Catal.* **1998**, *180*, 56–65. [[CrossRef](#)]
11. Jiang, J.; Lu, G.; Miao, C.; Wu, X.; Wu, W.; Sun, Q. Catalytic performance of X molecular sieve modified by alkali metal ions for the side-chain alkylation of toluene with methanol. *Microporous Mesoporous Mater.* **2013**, *167*, 213–220. [[CrossRef](#)]
12. Hong, Z.; Xiong, C.; Zhao, G.; Zhu, Z. Side-chain alkylation of toluene with methanol to produce styrene: An overview. *Catal. Sci. Technol.* **2019**, *9*, 6828–6840. [[CrossRef](#)]
13. Vadhri, V.M.; Hickey, T.; Mukherjee, M. Exelus Styrene Monomer (ExSyM) Process (Case Study). In *Industrial Arene Chemistry*; Wiley-VCH GmbH: Hoboken, NJ, USA, 2023; pp. 673–713.
14. Diaz, E.; Munoz, E.; Vega, A.; Ordonez, S. Enhancement of the CO₂ retention capacity of Y zeolites by Na and Cs treatments: Effect of adsorption temperature and water treatment. *Ind. Eng. Chem. Res.* **2008**, *47*, 412–418. [[CrossRef](#)]
15. Liu, H.; Oakland, N.J. Modified Zeolite Catalyst Composition and Process for Alkylating Toluene with Methanol to Form Styrene. U.S. Patent 4,499,318 A, 12 February 1985.
16. Unland, M.L. Infrared study of methanol decomposition on alkali metal X-type zeolites. *J. Phys. Chem.* **1978**, *82*, 580–583. [[CrossRef](#)]
17. Hong, Z.; Zhao, G.; Huang, F.; Wang, X.; Zhu, Z. Enhancing the side-chain alkylation of toluene with methanol to styrene over the Cs-modified X zeolite by the assistance of basic picoline as a co-catalyst. *Green Energy Environ.* **2022**, *7*, 1241–1252. [[CrossRef](#)]
18. Hong, Z.; Xiong, C.; Wang, X.; Huang, F.; Li, L.; Zhu, Z. Ammonia pools effect in Cs modified X zeolites for side-chain alkylation of toluene with methanol. *Chem. Eng. J.* **2023**, *474*, 145650. [[CrossRef](#)]

19. Zhang, Z.; Shan, W.; Li, H.; Zhu, W.; Zhang, N.; Tang, Y.; Yu, J.; Jia, M.; Zhang, W.; Zhang, C. Side-chain alkylation of toluene with methanol over boron phosphate modified cesium ion-exchanged zeolite X catalysts. *J. Porous Mater.* **2015**, *22*, 1179–1186. [[CrossRef](#)]
20. Zhang, Z.; Zhang, C.; Yuan, X.; Miao, S.; Li, H.; Shan, W.; Jia, M. Effect of Fe Additives on the Catalytic Performance of Ion-Exchanged CsX Zeolites for Side-Chain Alkylation of Toluene with Methanol. *Catalysts* **2019**, *9*, 829. [[CrossRef](#)]
21. Engelhardt, J.; Szanyi, J.; Valyon, J. Alkylation of toluene with methanol on commercial X zeolite in different alkali cation forms. *J. Catal.* **1987**, *107*, 296–306. [[CrossRef](#)]
22. Romero, M.D.; Ovejero, G.; Uguina, M.A.; Rodri'guez, A.; Gómez, J.M. Fast tailoring of the acid–base properties in the NaX zeolite by cesium-exchange under microwave heating. *Microporous Mesoporous Mater.* **2007**, *98*, 317–322. [[CrossRef](#)]
23. Hathaway, P.E.; Davis, M.E. Base catalysis by alkali modified zeolites: III. Alkylation with methanol. *J. Catal.* **1989**, *119*, 497–507. [[CrossRef](#)]
24. Nováková, J.; Kubelková, L.; Habersberger, K.; Dolejšek, Z. Catalytic Activity of Dealuminated Y and HZSM-5 Zeolites Measured by the Temperature-programmed Desorption of Small Amounts of Preadsorbed Methanol and by the Low-pressure Flow Reaction of Methanol. *J. Chem. Soc. Faraday Trans. 1 Phys. Chem. Condens. Phases* **1984**, *80*, 1457–1465. [[CrossRef](#)]
25. Chen, H.; Li, X.; Zhao, G.; Gu, H.; Zhu, Z. Free radical mechanism investigation of the side-chain alkylation of toluene with methanol on basic zeolites X. *Chin. J. Catal.* **2015**, *36*, 1726–1732. [[CrossRef](#)]
26. Yashima, T.; Sato, K.; Hayasaka, T.; Hara, N. Alkylation on synthetic zeolites: III. Alkylation of toluene with methanol and formaldehyde on alkali cation exchanged zeolites. *J. Catal.* **1972**, *26*, 303–312. [[CrossRef](#)]
27. Wieland, W.S.; Davis, R.J.; Garces, J.M. Side-Chain Alkylation of Toluene with Methanol over Alkali-Exchanged Zeolites X, Y, L, and β . *J. Catal.* **1998**, *173*, 490–500. [[CrossRef](#)]
28. Lin, D.; Zhao, H.M.; Zhang, X.Y.; Lan, D.X.; Chun, Y. Formation and Function of Formate in the Side-Chain Alkylation of Toluene with Methanol. *Chin. J. Catal.* **2012**, *33*, 1041–1047. [[CrossRef](#)]
29. Mielczarski, E.; Davis, M.E. Infrared investigations of the alkylation of toluene with methanol by alkali-modified zeolites. *Ind. Eng. Chem. Res.* **1991**, *29*, 288–291. [[CrossRef](#)]
30. Palomares, A.E.; Eder-Mirth, G.; Lercher, J.A. Selective Alkylation of Toluene over Basic Zeolites: An In Situ Infrared Spectroscopic Investigation. *J. Catal.* **1997**, *168*, 442–449. [[CrossRef](#)]
31. King, S.T.; Garces, J.M. In situ infrared study of alkylation of toluene with methanol on alkali cation-exchanged zeolites. *J. Catal.* **1987**, *104*, 59–70. [[CrossRef](#)]
32. Borowiak, M.A.; Jamróz, M.H.; Larsson, R. Catalytic decomposition of formic acid on oxide catalysts—An impulse-oscillation model approach to the unimolecular mechanism. *J. Mol. Catal. A Chem.* **1999**, *139*, 97–104. [[CrossRef](#)]

Disclaimer/Publisher's Note: The statements, opinions and data contained in all publications are solely those of the individual author(s) and contributor(s) and not of MDPI and/or the editor(s). MDPI and/or the editor(s) disclaim responsibility for any injury to people or property resulting from any ideas, methods, instructions or products referred to in the content.